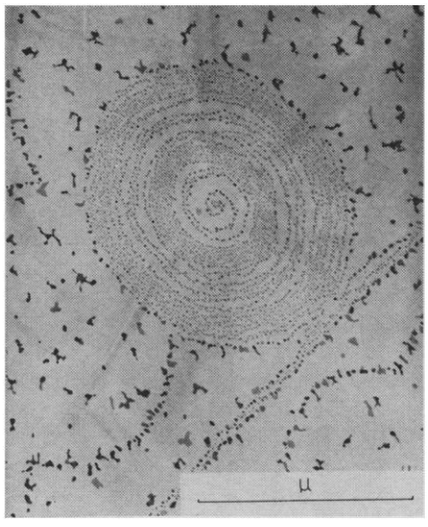

Fig. 1. Screw dislocation in "G.E." pyrographite, etched 46 minutes, CO_2, 1150°C.

surface steps are oxidized at an increasing rate, and thus the screw pattern is magnified (Fig. 1 and cover).

The magnitude of the Burgers vector (equal to pitch) of the screw can be determined by any procedure which measures the height of the step originating on the dislocation. For large steps which could, of course, be measured only by replication techniques, conventional shadowing techniques had been used (*3*). For monatomic steps, that is, steps which are only one atom layer high, the step height can most readily be demonstrated by creating additional surface steps known to be only one atom layer high, and etching the surface until the various steps merge. Monolayer steps can be created at will by any chemical or physical procedure which creates single vacancies. The most convenient one for the present problem was the creation of single surface vacancies by chemical attack with ozone. Detailed calibrations (*4*) had established that at 40°C a gas mixture of 10 percent ozone in oxygen created 10^{-6} surface vacancies per atom per minute and only negligible amounts of multilayer vacancies during the first hour of reaction.

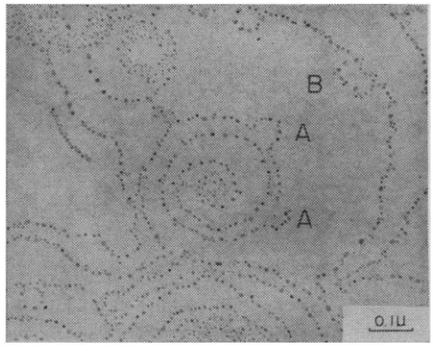

Fig. 2. Determination of Burgers vector. "French" pyrographite etched 24 minutes, CO_2, 1150°C; 1 minute, O_3, 40°C; 10 minutes, Cl_2–O_2, 650°C. *A*, Merged surface steps of dislocation and of loop. *B*, Nonmerging steps, indicating multilayer defect.

The cleaved crystals containing screw dislocations were, therefore, first etched in carbon dioxide to develop well-spaced screw steps, then treated with ozone to produce single surface vacancies, and finally etched briefly in a mixture of O_2 and Cl_2 to expand the vacancies into surface depressions large enough to guarantee frequent intersections with screw steps. An example of four such intersections is shown in Fig. 2. Two of the intersections, designated *A*, show true merging without any additional step between the loop and the screw. They demonstrate that the screw of Fig. 2 consists of a monatomic surface step, that is, a step 3.35 Å high, and that the *c*-component of the Burgers vector of the screw dislocation at the center of the screw is 3.35 Å. The intersection designated *B* shows an example of a multilayer step, which is, however, not part of a screw dislocation.

These methods have been applied thus far to three types of graphite. Natural graphite was obtained from the Ticonderoga area of northern New York State. This graphite is found both in igneous intrusion and in Precambrian limestone, in the form of crystals which are often of great perfection. Literally thousands of these have by now been examined by our group without revealing a single example of a monatomic screw dislocation. We estimate that we have searched at least 1 cm^2 so that an upper concentration limit of one screw per square centimeter is indicated. This estimate neglects the possible occurrence of isolated patches of screws, which could obstruct easy cleavage of the crystal and thus escape detection; nonetheless, patchy cleavage was rarely observed. The same crystals contain, however, an appreciable concentration of large screw dislocations (*3*) whose pitch is never less than 450 Å high, and which generate occasional spiral surface growth patterns (*3, 5*).

Pyrolytic graphite (*6*) had been recrystallized by heating above 3100°C under pressure. This material contained at least 5×10^8 screw dislocations, about equally left and right handed. Nearly all the screws which could be examined in detail had a pitch of one atom layer (Fig. 2). About five percent of the screws were very short, terminating within two or three layers. The concentration of screws may have exceeded $5 \times 10^8/cm^2$ because elongated crowded patches rendered precise determinations difficult.

A sample of pyrolytic graphite (*7*), which had been deposited at high supersaturation of carbon and subsequently had been heated in a graphite capsule at 3600°C, contained 10^6 screw dislocations per square centimeter.

Both samples of pyrographite were difficult to cleave and contained numerous defects other than the screw dislocations. The size and density distribution and the behavior of the screws on further annealing is still uncertain.

G. R. Hennig
Argonne National Laboratory, Argonne, Illinois

References and Notes

1. G. R. Hennig, *Appl. Phys. Letters* **4**, 52 (1964).
2. ———, *J. Chem. Phys.* **40**, 2877 (1964).
3. ———, *J. Chim. Phys.* **12** (1961); G. R. Hennig and M. A. Kanter, *Proc. Intern. Symp., Reactivity Solids*, 4th Symposium, J. H. DeBoer, Ed. (Elsevier, Amsterdam, 1960), p. 649.
4. G. R. Hennig, in preparation.
5. F. H. Horn, *Nature* **170**, 581 (1952).
6. Furnished by J. Maire, Carbone Lorraine, France, and described by J. Maire, *Carbon* **1**, 357 (1964).
7. Furnished by R. Diefendorf of General Electric, Schenectady, N.Y.
8. Work performed under auspices of AEC.

9 December 1964

Electron Microprobe Analysis of Oxygen in an Iron Meteorite

Abstract. *A quantitative analysis of oxygen in the iron-nickel matrix of the Santa Catherina iron meteorite has been accomplished by using an electron microprobe with dispersive x-ray optics and by applying theoretically calculated corrections to the observed intensity ratios. Microvolume analyses and two-dimensional scanning images in OKα, FeLα, and NiLα x-radiation show that the high nickel phase of the meteorite has been oxidized while the low nickel phase has remained unoxidized.*

The Santa Catherina iron meteorite is a nickel-rich ataxite with an overall nickel content of 36.14 percent by weight (*1*). Considerable importance has been attached to this meteorite because it appears to have originally consisted of two coexisting iron-nickel alloys of the high nickel γ-phase (*2*) which have not been found in other iron meteorites or man-made alloys. Polished sections

of the meteorite show two major phases which vary considerably in their relative abundances from place to place in the meteorite. By means of an electron microprobe x-ray analyzer (*3*), we have made quantitative analyses of the oxygen in these two phases. This accomplishment is important because until recently (*4*) the electron microprobe, which performs a nondestructive, chemical analysis of micron-sized volumes of the surface regions of a solid sample (*5*), was limited to analyses of elements of atomic number 12 or greater (x-ray wave lengths $\leqq$ 10 Å). New techniques, however, now permit the detection of x-rays up to 93 Å in wavelength (*6*). The range to 93 Å includes the K spectra of all elements through boron as well as the L spectra of the transition metals.

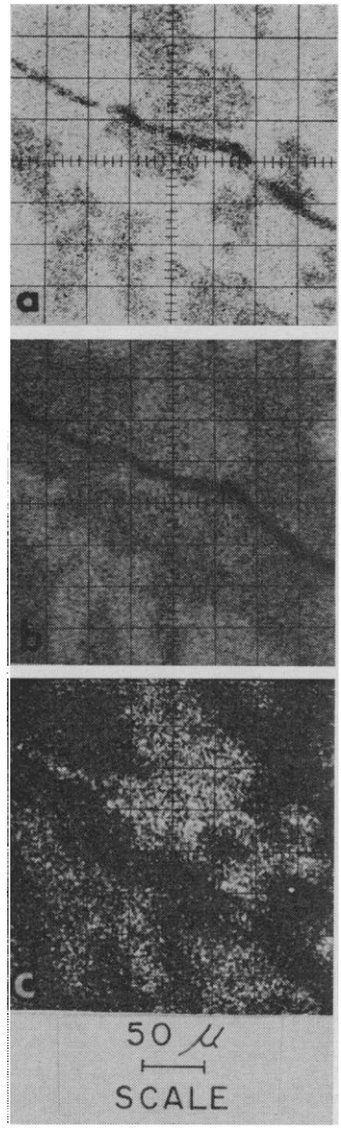

Fig. 1. FeLα, NiLα, OKα x-ray scanning photographs of the Santa Catherina iron meteorite. (Phase I, low nickel concentration; phase II, high nickel concentration.) Accelerating voltage, 5 kv.

Table 1. Electron microprobe analyses of the Santa Catherina iron meteorite. For the complete analyses of phase II, samples were removed from obvious cracks in the meteorite.

Element	Preliminary analysis		Complete analysis
	Phase I (wt %)	Phase II (wt %)	Phase II (wt %)
Fe	67.3	46.1	46.1
Ni	31.8	45.2	45.2
Co	0.63	0.63	0.63
P	< 0.1	< 0.1	< 0.1
O			8.4
Total	99.8_8	91.9_8	100.3_8

In a preliminary study with an electron microprobe, there were indications that two compositionally distinct phases existed in this iron meteorite (Table 1), the main dark-etching phase (phase I) containing less nickel than the unevenly distributed light-etching phase (phase II). The analysis of phase I (Table 1) indicated that all major elements had been accounted for, but in phase II, some 8.1 percent by weight of the phase was missing and was interpreted as being attributable to one or more elements with atomic numbers less than 12. We have now made a complete (atomic number greater than 4) spectrum analysis and have found that, except for the elements already determined (Table 1), oxygen is the only major element present in a concentration greater than 1 percent.

Excellent x-ray scanning photographs were obtained with OKα radiation (23.707 Å) after exposures of about 1 hour, a potassium acid phthalate (KAP) analyzer crystal and a flow proportional counter being used with a supported, nitrocellulose window, 2000 Å thick. Figure 1 shows the distribution of oxygen in the Santa Catherina iron meteorite. X-ray scanning pictures were also taken with FeLα radiation (17.602 Å) and with NiLα radiation (14.595 Å), to show the distribution of iron and nickel, respectively, in the same area (Fig. 1). From these photographs it was obvious that the component of low atomic weight in the nickel-rich phase II was, in fact, oxygen and that this phase had apparently been selectively oxidized by terrestrial oxidation along cracks in the meteorite while the main groundmass, phase I, had remained unoxidized.

Quantitative oxygen analyses of phase II were made with a 5-kv accelerating potential on the primary electron beam. A homogeneous specimen of magnetite (Fe_3O_4) was used as a standard. No corrections were required for wavelength shift and, because of the low counting rates, detector dead time corrections were not necessary. Background measurements were made on areas of oxygen-free phase I and on samples of pure Fe. Mass absorption corrections for OKα in FeNi were made by assuming the mass absorption coefficient for Fe to be 24,000 and for Ni to be 25,500. These values were extrapolated from data given by Henke *et al.* (*7*). Green's (*8*) experimental f (χ) curves for CKα were used to interpolate the 5-kv curve which was used in conjunction with these mass absorption coefficients to derive an absorption correction factor of 1.177. No correction for secondary fluorescence was required. Corrections for atomic number were not made because of the possibility of large errors in the estimated mass absorption coefficients. The chemical similarity of the standard and the sample would also tend to make this correction very small. An outline of the corrections is given in Table 2 as they apply to the oxygen contents measured on phase II as a function of the distance from the oxidized crack shown in Fig 1.

The complete analysis (Table 1) of phase II as it occurs in our samples of the Santa Catherina iron meteorite removed from obvious oxidized cracks explains in full the low total weight

Table 2. Calculation of the oxygen content of phase II.

Sample	Observed counts		Oxygen content (wt %)	
	OKα	Background	Relative to magnetite standard	After absorption correction
Magnetite standard*	341	19		
Phase II				
Removed from crack	102 (27)†	19	7.1	8.4
Close to crack	133 (4)	19	9.8	11.5
Very close to crack	186 (6)	19	14.3	16.9

* 27.6 percent oxygen. † Numbers in parentheses indicate the number of individual analyses made.

percent found in the preliminary analysis (Table 1) and demonstrates the power of the electron microprobe in making accurate analyses of the abundances of the light elements.

J. F. LOVERING
Department of Geophysics, Australian National University, Canberra
C. A. ANDERSEN
Hasler Research Center, Applied Research Laboratories, Inc., Goleta, California

Reference and Notes

1. Analyzed by A. J. Easton.
2. J. F. Lovering and L. G. Parry, *Geochim. Cosmochim. Acta* **26**, 361 (1962).
3. Applied Research Laboratories, Glendale 8, Calif.
4. J. Merritt, C. E. Muller, W. M. Sawyer, Jr., A. Telfer, *Anal. Chem.* **35**, 2209 (1963); C. A. Andersen, K. Keil, B. Mason, *Science* **146**, 256 (1964).
5. R. Castaing, in *International Symposium on X-Ray Optics and X-Ray Microanalysis, 3rd, Stanford University, 1962*, H. H. Pettee, V. E. Cosslett, A. Engstrom, Eds. (Academic Press, New York, 1963), p. 263–277.
6. E. Davidson, W. E. Fowler, H. Neuhaus, W. G. Shequen, paper presented at the 1964 Pittsburgh Conference on Analytical Chemistry and Applied Spectroscopy, 6 March 1964, Paper No. 188.
7. B. L. Henke, R. White, B. Lundberg, *J. Appl. Phys.* **28**, 98 (1957).
8. M. Green, in *International Symposium on X-Ray Optics and X-Ray Microanalysis, 3rd, Stanford University, 1962*, H. H. Pettee, V. E. Cosslett, A. Engstrom, Eds. (Academic Press, New York, 1963), p. 361–377.

30 October 1964

Anomalous Abundance of Upper Atmosphere Sodium, 1964

Abstract. *Measurements of atomic sodium in the upper atmosphere by absorption spectroscopy with the Pepsios spectrometer on the Fraunhofer D_2 line during February to August 1964 at Madison, Wisconsin, have indicated abundances of about $10^{10}/cm^2$ for the late winter, about twice the values from a similar method in 1961–62. An abrupt decrease in abundance occurred during March in agreement with established seasonal behavior, but the abundance then increased anomalously in the summer to $8 \times 10^9/cm^2$. The summertime increase may be related to observations of increased turbidity of the upper atmosphere, presumably caused by volcanic dust.*

The abundance of atomic sodium in the atmosphere during recent years has been determined spectroscopically from emission measurements on the twilight glow, in dayglow and twilight glow with the Zeeman-effect photometer, in absorption with a sodium scattering cell, and by absorption of direct sunlight with the Hypeac grating-Fabry-Perot spectrometer at high resolution. The complex problem of the annual variation of abundance, with its probable dependence upon geographic location, appears unsolved. Much of the accumulated evidence points to a seasonal variation marked by a late winter maximum and rapid springtime decrease to a summer minimum and slow autumn increase (*1*); but a recent extensive compilation based mainly upon Zeeman-effect photometry points to a summer maximum (*2*).

It is not my purpose in this report to contribute data on the general problem of the annual abundance, but rather to describe a particular anomaly observed at one place in 1964, compare it with the most nearly comparable previous data, and point out a correlation—convincing to me—with an atmospheric disturbance that offers a clue to the origin of at least that sodium which contributes to the anomaly.

The terrestrial absorption associated with the Fraunhofer D_2 line from February to August 1964 at Madison, Wisconsin, was observed with a Pepsios spectrometer (*3*), an instrument particularly suitable for work on this problem because of great luminosity at high resolution in a dense spectrum and the simple interpretability of the output. The observations are compared with those made in a similar manner during 1961–62 by McNutt (*4*) with a Hypeac. Figure 1 is a representative Pepsiogram of the D_2 line. Reduction of the data was accomplished and corrected to vertical abundance (*4*). The method is rather insensitive to the altitude of the layer, here taken to be 85 km.

The 1961–62 and 1964 seasonal variations are shown in Fig. 2. The springtime abundances decrease abruptly during March in both 1962 and 1964, but the 1964 abundance is clearly about twice that of 1962. Systematic errors, especially in determining the no-absorption contour of the line, might have shifted the 1964 abundance points upward, but by not more than about 20 percent.

In recent months visual and photometric observations have been made elsewhere indicating that volcanic dust has been accumulating in the upper atmosphere, reaching the northern hemisphere in the autumn of 1963 (*5*). I suggest that the high 1964 summertime abundance of atomic sodium is a direct consequence of the large amount of volcanic dust, which serves in this instance as the primary source of the increased sodium. The dust layers have been observed to be at 20 km and higher. The spectroscopic observations reported upon here are not sufficiently sensitive to zenith angle to determine the height of the absorbing layer, but consideration of collisional and Doppler broadening and the observed resolution of the 57-mK(millikayser) hyperfine struc-

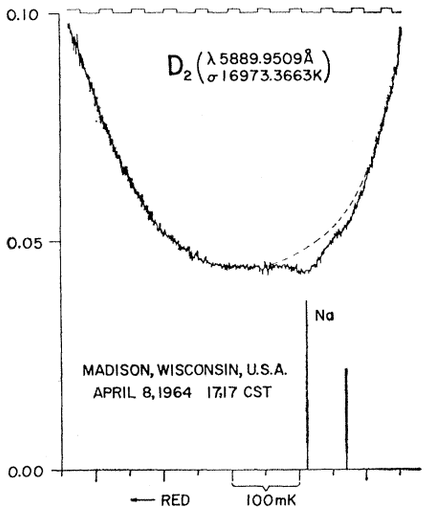

Fig. 1. Pepsiogram of the bottom of the Fraunhofer D_2 absorption line of the solar spectrum. The terrestrial sodium is identified by its position relative to the solar line, which has a gravitational red shift plus a Doppler shift, and by resolution of the two hyperfine structure blends which are observable by virtue of the low pressure and temperature of the upper atmosphere. Ordinate, intensity (continuum ≡ 1.00); abscissa, wave number (50 mK per division).

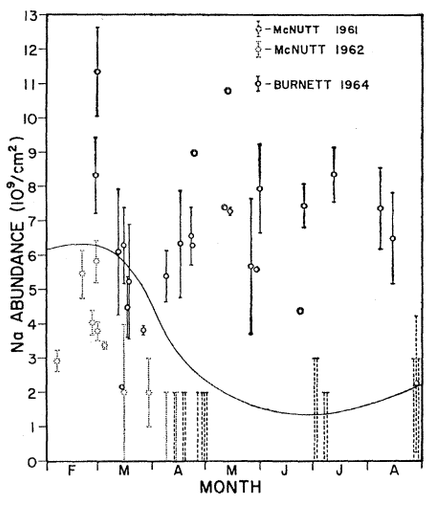

Fig. 2. Abundance of atomic sodium in the atmosphere at Madison, Wisconsin (43° N). Daily averages for 1961–62 and 1964 are shown with vertical lines indicating one standard deviation. Circles without vertical lines are single measurements. The curve is a seasonal curve for Saskatoon, Saskatchewan (52°N).